Annals of R.S.C.B., ISSN:1583-6258, Vol. 25, Issue 3, 2021, Pages. 7841 - 7852
Received 16 February 2021; Accepted 08 March 2021.

Multi Model Clustering Segmentation and Intensive Pragmatic Blossoms (Ipb) Classification Method based Medical Image Retrieval System

R. Inbaraj [1], Dr.G.Ravi[2]

[1] Research Scholar, Department of Computer Science, Jamal Mohamed College (Autonomous), [Affiliated to Bharathidasan University], Tiruchirappalli – 620020, India.

[2] Head & Associate Professor, Department of Computer Science, Jamal Mohamed College (Autonomous),
[Affiliated to Bharathidasan University], Tiruchirappalli – 620020, India.

ABSTRACT:

Nowadays, medical images are generated more and more in their daily activities, which are in millions of sizes. Retrieving medical images from an extensive collection is then a daunting task from a content-based medical image retrieval system (CBMIR) system. Until the extraction of the disease by automated segmentation calculates the bottleneck based on medical image search material. Before that, a few approaches are based on one-to-one image grains that are still sensitive to rotation and expansion. In this work, to address the last problems, introduce Multimodal Clustering Segmentation (MCS)and Intensive Pragmatic Blossoms (IPB) Classification method for medical image retrieval system. Compared to other conventional medical image retrieval, the proposed MCS and IPB method gives a good result. Theoverall retrieval efficiency of the proposed method is 97.23%

Keywords: Unsupervised Vector Zone Feature Extraction,Intensive Pragmatic Blossoms, clustering, precision, F-Measure

1. INTRODUCTION

Clustering-based image classification is one of the issues experienced in PC appearance and image handling. It works straightforwardly in certain zones of the Human Visual System (HVS). However, in data frameworks, it just works under specific presumptions and impediments. Clustering can be separated by their hardness, perfection, direction, designing, and so on. Indeed, even hues can be sensitive.The clustering classification include has been improved by adding shading data to the extraction stage. Classification is fundamental in clustering content-based image retrieval (CBIR) applications, remote detecting applications, and numerous regions.

A major revolution in digital imagery [1] occurred in the last years. These images are presented in broad use and profoundly utilized in down-to-earth life; Medicine is one of the most significant and shared ones. These images have a ton of criticalness since they reflect and incorporate primary and significant data identified with numerous pieces of the body. This data would then be utilized in procedures, for example, malady identification, clinical training, and specialists [2]. With current turns of events, medical images would now be made by emergency

Annals of R.S.C.B., ISSN:1583-6258, Vol. 25, Issue 3, 2021, Pages. 7841 - 7852
Received 16 February 2021; Accepted 08 March 2021.

clinics, clinical focuses [3], and pharmaceutical organizations. Therefore, there is a need to navigate the techniques and create this vast number of medicine imagesto get an accurate search. Returning the traditional image depends on the placement and searches of the table for manually assigning images to words. Like this, the meaningful images can be determined dependent on the words included; this technique is called Text-based image retrieval (TBIR) [4-5].

Consequently, the analysts started to utilize content-based image retrieval (CBIR), which is the strategy for image retrieval and the image's visual substance. Low-level highlights, for example, shading, piece, and shape,are naturally removed to scan for images related to the question image, dependent on the noticeable substance initially. CBIR methods are quicker than utilizing ordering and retrieval strings [6]. In any case, CBIR frameworks can't decipher the information in a significant level semantic idea utilized by humans to recognize images. These are called semantic spaces [7]. Semantic space is characterized as a space between the PC's components to group images and low-level highlights, significant level semantic ideas to order how human creatures comprehend an image. Along these lines, there is a provoking issue to lessen semantic space by PCs where significant level semantic thoughts can be disengaged from the human eye [8]

As of late, analysts have endeavored to utilize clinical image classification to care for a subject space issue. Image classification is considered alongside writings in image semantic substance; this procedure is without a doubt basic and middle in recovering images [9-10]. Machine learning procedures have been, as of late, utilized in image classification frameworks, for the most part, to get elevated level semantic ideas from visual highlights [11]. Numerous advantages can be accomplished with clinical imaging, which X-beam portrays; Diagnosis, Researchers and Practice, for showing purposes, clinical notes and careful arranging.GLCM is a conventional right top-end include extraction, image recognition [12], image segmentation [13], image retrieval [14], and image classification [15], and valuable for amalgamation investigation strategies [16-17].

2. PROPOSED MATERIALS AND METHOD FOR CLUSTERING IMAGE CLASSIFICATION:

This section discusses the working function of the proposed content-based medical image retrieval system. Through this work, doctors can be of great help in medical care and research.Take care of that difference once this method is needed. Before analyzing trends, we first extract the model's features to extract specific features such as requirements models and color functions that can be used to create parts with all images of the specific position held where the noise and unwanted data are found to be too high for use. Finally, in this classification category, a new image can predict medical images.

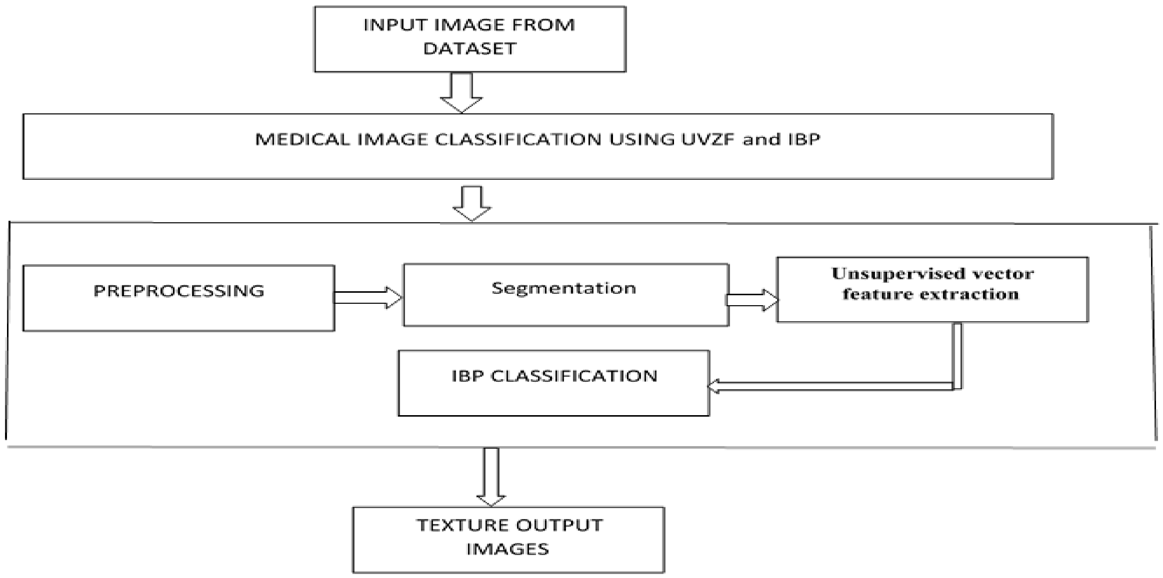

Figure 1: Block Diagram of Proposed Materials and Method

2.1 PREPROCESSING USING GABOR FILTER

In the preprocessing phase, we create values for the grayscale of the original image. The generated grayscale values are then imaged with the uniform gray distribution, normalized with the gray value distribution. In this work,the Gabor filter is used for preprocessing. The proposed method generates image map values. We will use a 64-bit map for our purpose if the resulting value segmentation procedure is used. You have categorized the image based on the result by graph balancing. The resulting image will be displayed to the user and not allowed to provide a new drawing. The compilation process is entered based on the original size, and the segmentation process is entered to give a new result. This method stays on the accelerator until the user is satisfied.

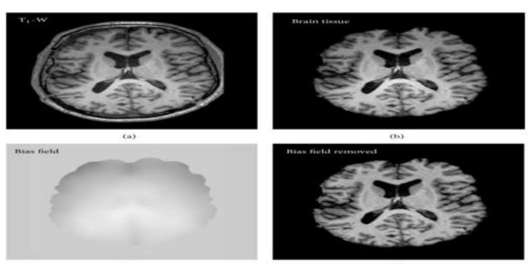

Figure 2: Result of Preprocessing

2.2 MULTI MODEL CLUSTERING SEGMENTATION

The image developed in the feature extraction phase has been chosen for segmentation. This work uses multi-model clustering segmentation. From the image, every pixel hub is chosen. Its energy is evaluated utilizing the dark estimation of the pixel and area dim mean of the pixel processed in the prior stage. The force esteem shows how well a pixel conveys the feature of

Annals of R.S.C.B., ISSN:1583-6258, Vol. 25, Issue 3, 2021, Pages. 7841 - 7852
Received 16 February 2021; Accepted 08 March 2021.

neighboring pixels. A pixel will be appointed to a cluster just if the energy factor is inside the edge of energy components of pixels present in the gathering. Segmentation is performed utilizing registered energy factors and will be iterated till the client gets fulfilled.

2.2.1 ALGORITHM MULTI MODEL CLUSTERING SEGMENTATION:

Input: Image F, the number of clustering k

Output: Clustering results R

Steps and process:

Step1: Acquire the histogram H of image F;

Step2: Make histogram equalization to H using H;

Step3: Make clustering;

Step4: Generate k clustering center;

4.1 Set i=1;

4.2 If not null, select a data point regarded as the i^{th} clustering center

Else, go to step4.1;

4.3 If i<k,i++,return step 4.2

Else, go to step 3;

4.4 If null, find the k-i+1clustering center; else return;

Step5: Computing the distance between each sample t with each cluster center;

Step6: selecting the nearest clustering center;

Step7: Computing the objective function

Step8: If the function is convergence, the algorithm is finished;

Step9: Computing the clustering center k according to step4

2.3 FEATURE EXTRACTION: UNSUPERVISED VECTOR ZONE FEATURE EXTRACTION

After segmentation, the Feature esteems are extricated dependent on the comparability proportion of every pixel grouping at various zones. The inspiration for utilizing multiple zones (inside, limit, and encompassing sore) and the picked features depends on how the kind-hearted injuries differ from the dangerous sore by their inside, fringe, and encompassing tissue attributes. In dangerous injuries, the inward injury structure shows a broad scope of changes (heterogeneous lessening) and neighboring structures' attacks. A thick upgrading edge encircles the clustering;

Annals of R.S.C.B., ISSN:1583-6258, Vol. 25, Issue 3, 2021, Pages. 7841 - 7852
Received 16 February 2021; Accepted 08 March 2021.

the injury fringe is characterized as sporadic or not well-characterized edges. Be that as it may, the inside structure is diffusely homogeneous, with a slim or missing edge; the sore fringe is the round or oval form with a sharp edge.In this work,12 features were extracted for the proposed technique. A few of them are described as follows.

Energy

The energy also measures the second-order statistical parameter: the textural consistency and the pixel pair repeats. The maximum energy of the structure or image occurs when the gray level distribution of a particular image is either constant or uniform

$$Energy = \sum_{i,j=0}^{N-1} (pi,j)^2 \quad \dots (1)$$

Where

Pij =ijthentry of the normalized co-occurrence matrix, N = Number of pixels.

Contrast

Contrast is a measure of the difference in brightness, making the value traceable. Range = [0, 1].

$$Contrast = \sum_{i,j=0}^{N-1} pi,j(i-j)^2 \dots (2)$$

Where

N-1 = Dimension value for the total number of pixels, Pij = Color Values.

Correlation

The connection between the neighbor pixels is evaluated using correlation with the range of= [-1, 1].

$$Correlation = \frac{(N\sum xy)-(\sum x)(\sum y)}{\sqrt{[N\sum x^2-(\sum x^2)][N\sum y^2-(\sum y^2}} \dots (3)$$

Where:

N= Image Count, $\sum xy$= Mean value of the Paired image

$\sum x$= Mean value of image x, $\sum y$= Mean value of image y

$\sum x^2$= Squared mean value of x image, $\sum y^2$= Squared mean value of y image

Homogeneity

The component propagates homogeneity measures in the MGRLBP close to the MGRLBP diagonal. Range= [0, 1]

Annals of R.S.C.B., ISSN:1583-6258, Vol. 25, Issue 3, 2021, Pages. 7841 - 7852
Received 16 February 2021; Accepted 08 March 2021.

$$\text{Homogeneity} = \sum_{i,j=0}^{N-1} \frac{pij}{1+(i-j)^2} \dots (4)$$

Where

i and j = pixel

pij = Pixel value.

Mean

The mean called the intermediate frequency value is multiplied by the sum of all values with the total number of occurrences. The pixel value event is only its frequency, but some neighboring pixel value is only the event frequency.

$$\boldsymbol{Mean} = \sum_{i=0}^{G-1} \sum_{j=0}^{G-1} \boldsymbol{ip}(\boldsymbol{i},\boldsymbol{j}) \dots (5)$$

Skewness

The skewness is a measure of nonlinearity, and its meaning is to measure the probability distribution of a random variable. The similarity of chromatin is measured via skewness. The skewness value can be either positive or negative or undefined. The formula of skewness as

$$\boldsymbol{Sk} = \sum_{i=1}^{N} \frac{(x_i-\bar{x})^3/N}{y^3} \dots (6)$$

Where

$\bar{x}$ = mean value , y= value of standard deviation, N = data point numbers

Kurtosis

Height and sharpness are measured by the sum of the remaining relative magnitudes of a number called kurtosis. High values indicate a higher sharper peak, but lower values indicate a lower-less distinct peak. Thus, more sensitive evaluations of biological images can also be characterized by chromatin.

$$\boldsymbol{Ku} = \frac{\sum_{i=1}^{N}(\mu_i-\mu)^4/N}{S^4} \dots (7)$$

μ = mean value,S= value of standard deviation, N = data point numbers

Standard Deviation

The square root of the image is a standard deviation. The variance value is defined as the intensity variation around the mean value of the image. The standard deviation is more minor if the value of the variance is closer to the mean

$$\boldsymbol{SD} = \sqrt{\frac{\Sigma|x-\mu|^2}{N}} \dots.. (8)$$

Annals of R.S.C.B., ISSN:1583-6258, Vol. 25, Issue 3, 2021, Pages. 7841 - 7852
Received 16 February 2021; Accepted 08 March 2021.

Where

x= image's thickness value, $\boldsymbol{\mu}$ = Value of mean, N = data point number

Variance

The average value of the variance p(i, j) places relatively high weights on the varying components. It refers to the variability of the gray level of the pixel pairs and the computation of the polynomial. Variance increases when gray-level values differ by their means.

$$\boldsymbol{Var} = \sum_{i=0}^{G-1} \sum_{j=0}^{G-1} (\boldsymbol{i} - \boldsymbol{\mu})^2 \, \boldsymbol{p}(\boldsymbol{i}, \boldsymbol{j}) \ \dots (9)$$

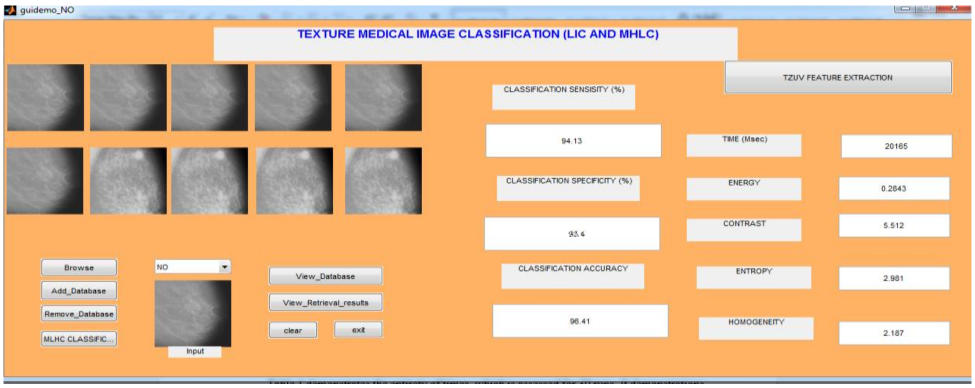

Figure 3: Clustering Feature Extraction of Mammography Image

The above figure demonstrates clustering feature extraction parameters screen on mammography images by using the UVZF method.

2.4 DEEP CONVOLUTIONAL INTENSIVE PRAGMATIC BLOSSOMS (IPB) CLASSIFICATION

The classifier is utilized to characterize average images from a database. For effortlessness, a solid expanded bloom classifier is utilized here. IPB is to make clinical images isolate two classes with the most extreme hole between them in our proposed framework yield of segmentation as a contribution to concentrated even-minded blooms classifier, which takes preparing information. To measure the presence of classification, we directed five unique arrangements of examinations. In the first round of tasks, we utilized 30% of the examples of each class of the dataset to make class delegate vectors (preparing) and the staying 70% of the examples for testing reason. The extra arrangement of trials is with preparing and testing tests in the proportion 40:60, 50:50, 60:40, and 70:30 individually. In each set, tests are rehashed multiple times by picking the preparation tests arbitrarily. For IPB, we chose the tissues esteem observationally. During experimentation, we break down 20 preliminaries for each arrangement of preparing and testing tests haphazardly.

2.4.1 INTENSIVE PRAGMATIC BLOSSOMS (IPB) ALGORITHM:

The Intensive Pragmatic Blossoms (IPB) algorithm is as follows: -

Step 1: Read the intensity corrected image.

Annals of R.S.C.B., ISSN:1583-6258, Vol. 25, Issue 3, 2021, Pages. 7841 - 7852
Received 16 February 2021; Accepted 08 March 2021.

Step 2: An enhanced image of the related image for preprocessing.

Step 3: Calculate each iteration of the anisotropic diffusion of the threshold

$$T = \max(r(T)) \ldots . (10)$$

i. Where r(T) =E(X'-X), where X is the image and X' is the generalized defeat identification.
ii. Perform directional anisotropic diffusion
iii. If convergence is reached, go to step 3. Otherwise, repeat step 2.

Step 4: output de-noised image

Step 5: The error in the output layer is back-propagated, and the error between the expected output Sk and ZK output is calculated by:

$$E_k = Z_k(Z_{k-1})(s_k - Z_{k)} \ldots (11)$$

the error calculation propagation is hidden on this layer using the following formula:

$$\frac{dx}{dt} = \mathrm{ATg(Fj)Fj} \ldots (12)$$

Step 6: Fixed connection weight correction between the input layer and a hidden layer

$$DW_{ji} = nX, Fj \ldots (13)$$

Where

DW_{ji} = The weight connection between layers of an image

x = Image intensities and function Fj is used to prevent blurring over edges and

$$DY_o = nx, fj \ldots (14)$$

DY_o is the after removing blurring images nx is the intensities function.

Then change the connection between the input layer and the output layer:

$$DW_{kj} = nyjE_k \ldots (15)$$

N is a parameter to be determined empirically.

Where E_k this energy may be written as the steady-state optimization of the energy functional

Step 6: Loop to st until a stop to define criterion (varied the number clusters).

Step 7: end

The classification's exhibition has been assessed concerning classification exactness, accuracy, review and F-measure from the classification's disarray network. The estimations have

Annals of R.S.C.B., ISSN:1583-6258, Vol. 25, Issue 3, 2021, Pages. 7841 - 7852
Received 16 February 2021; Accepted 08 March 2021.

been processed by utilizing the conditions depicted beneath with the accompanying conventions.TP (True Positive) =Positive units named positive. Careful Negative (TN) = Negative examples delegated negative. FP (False Positive) = Negative examples named positive. FN (False Negative) = Positive examples delegated negative

4. RESULTS AND DISCUSSION:

This section shows the simulation results and empirical performance evaluation of the proposed content retrieval strategy to retrieve the underlying medical images. Attempts were made on medical datasets collected to test the proposed technique for detailed experimental studies. The proposed work simulation is developed using Matlab simulation software.

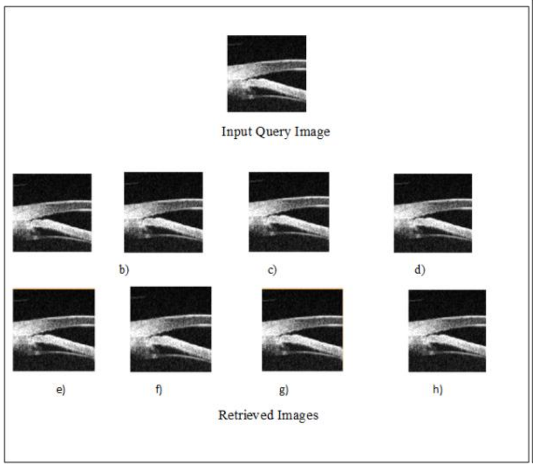

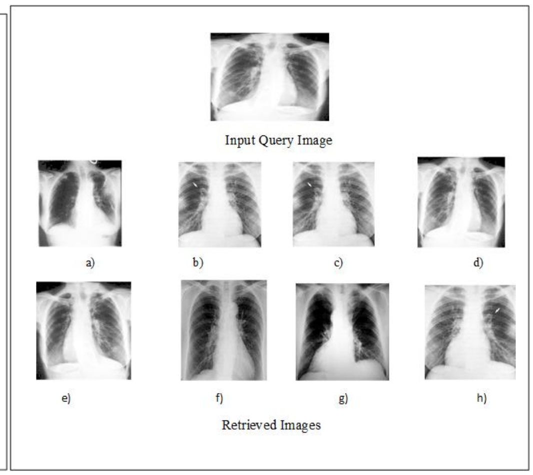

a) Result of Bone Images b) Result of Chest Images

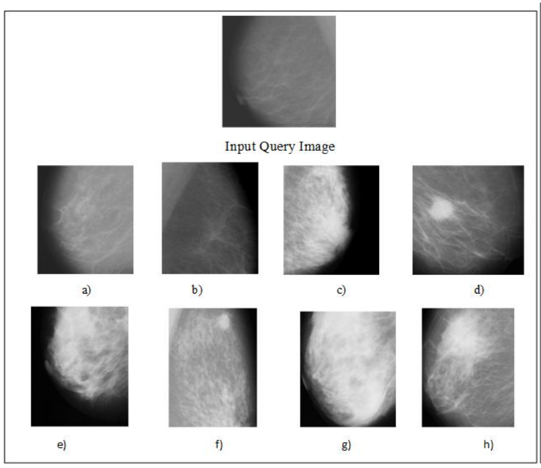

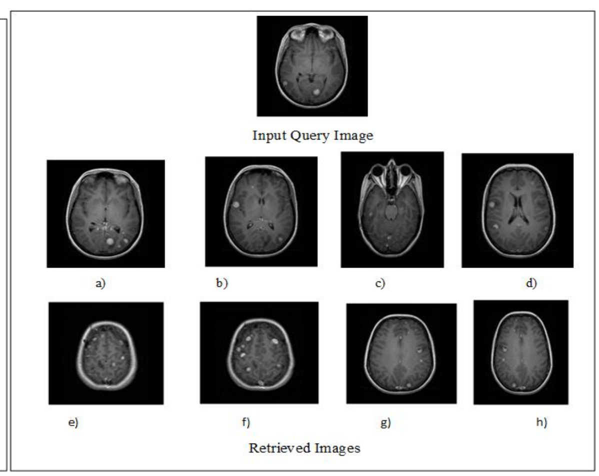

c) Result of Mammogram Images d) Result of MRI Brain Images

Figure 4. Simulation results of the bone retrieved image

Figure 4shows the simulation result of the proposed content-based medical image retrieval system. These results show the different medical datas of the human bone image, chest image, and mammogram image and brain images.

Annals of R.S.C.B., ISSN:1583-6258, Vol. 25, Issue 3, 2021, Pages. 7841 - 7852
Received 16 February 2021; Accepted 08 March 2021.

Table 1. Performance analysis of the proposed system with existing methods

S.no	Parameters	SVM [Kabbur et.al 2016]	ANN[Kabbur et al. 2016]	Proposed Method
1	Precision	93.02	94.56	96.32
2	Recall	89.03	90.89	92.93
3	F-measure	12.63	10.30	5.765
4	Accuracy	94.98	96.59	97.23

Table 1 talk about the Performance examination of the proposed content-based clinical image retrieval framework with existing substance-based clinical image retrieval techniques. This examination expresses that the proposed UVZF and IPB classifier content-based clinical image retrieval framework accomplishes the best outcome.

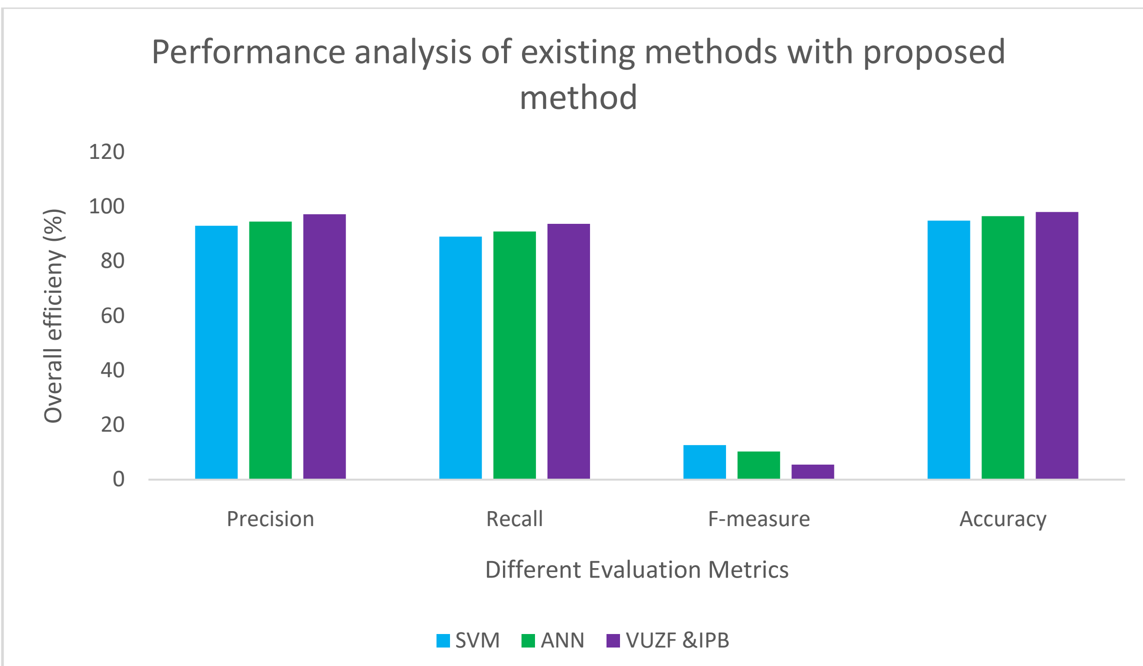

Figure 5. Performance analysis of proposed system

Figure 5 talk about the Performance examination of the proposed content-based clinical image retrieval framework with existing substance-based clinical image retrieval strategies. This correlation plainly expresses that the proposed content-based clinical image retrieval framework accomplishes the best outcome. For instance, the general exactness, overall precision, recall, F-measure, and proposed system accuracy are 96.32%, 92.93%, 5.76%, and 97.23% separately.

5. CONCLUSION

This work has proposed a new method of content-based medical image retrieval called Unsupervised Vector Zone Feature extraction and Intensive Pragmatic Blossoms classifier to retrieve familiar medical images. Many algorithms, frameworks and systems have been developed to search for help through large multimedia databases based on the study's content. Because of the importance of drafting medical physics, there has recently been an increasing interest in informative researchers and clinicians to create frameworks for CBIR algorithms and clinical image applications. But the strategies to overcome the existing work drawbacks. The simulation of the proposed work is developed using MatLab simulation software. The exhibition of the technique anticipated in this work is empowering. The proposed strategy is goodcompared to the strategies portrayed in literature, in light of the presentation measurements in particular precision, recall, F-measure. For example, the overall precision, recall, F-measure and accuracy of the proposed system are 96.32%, 92.93%, 5.76%, and 97.23%, respectively.

REFERENCES:

1. K. Egerer, d. Roggenbuck, r. Hiemann, m. G. Weyer, t. B̈uttner, b. Radau, r. Krause, b. Lehmann, e. Feist, and g. R. Burmester, "automated evaluation of autoantibodies on human epithelial-2 cells as an approach to standardize cell-based immunofluorescence tests, " arthritis research and therapy, vol. 12, no. 2, p. R40, 2010.
2. N. Doshi and g. Schaefer, "automatic classification of hep-2 cells using multi-dimensional local binary patterns," in 2nd iaprasian conference on pattern recognition, 2013.
3. Cheng, Ching-Hsue& Liu, Wei-Xiang. (2018). Identifying Degenerative Brain Disease Using Rough Set Classifier Based on Wavelet Packet Method. Journal of Clinical Medicine. 7. 124. 10.3390/jcm7060124.
4. Purcaru MAP, Repanovici A, Nedeloiu T. Non-Invasive Assessment Method Using Thoracic-Abdominal Profile Image Acquisition and Mathematical Modeling with Bezier Curves. J Clin Med. 2019;8(1):65. Published 2019 Jan 9. doi:10.3390/jcm8010065
5. Miranda, E.; Aryuni, M.; Irwansyah, E. A survey of medical image classification techniques. In Proceedings of the IEEE International Conference on Information Management and Technology, Bandung, Indonesia, 16–18 November 2016; pp. 56–61
6. Wan, Ji& Wang, Dayong& Hoi, Steven & Wu, Pencheng& Zhang, Jianke& Li, Jintao. (2014). Deep Learning for Content-Based Image Retrieval: A Comprehensive Study.
7. Yu, Dong & Deng, li. (2011). Deep Learning and Its Applications to Signal and Information Processing [Exploratory DSP]. Signal Processing Magazine, IEEE. 28. 145 - 154. 10.1109/MSP.2010.939038.
8. Litjens G, Kooi T, Bejnordi BE, A survey on deep learning in medical image analysis, Medical Image AnalysisVolume 42, December 2017, Pages 60-88

9. Kabbur, Mahabaleshwar. (2016). An Efficient Multiclass Medical Image CBIR System Based on Classification and Clustering. Journal of Intelligent Systems. 27. 10.1515/jisys-2016-0156.
10. P. Foggia, g. Percannella, p. Soda, and m. Vento, "benchmarking hep-2 cells classification methods, " ieee-tmi, 2013
11. S. Liao, m. Law, a. Chung, "dominant local binary patterns for clustering classification", ieee trans. Image process., vol. 18, no. 5, pp. 1107-1118, may 2009.
12. J. Ren, x. Jiang, j. Yuan, "noise-resistant local binary pattern with an embedded error-correction mechanism", *ieee trans. Image process.* vol. 22, no. 10, pp. 4049-4060, oct. 2013.
13. Z. Guo, l. Zhang, d. Zhang, "a completed modeling of local binary pattern operator for clustering classification", ieee trans. Image process. vol. 19, no. 6, pp. 1657-1663, jun. 2010.
14. F. Khellah, "clustering classification using dominant neighborhood structure", *ieee trans. Image process.*, vol. 20, no. 11, pp. 3270-3279, nov. 2011.
15. T. Song, f. Meng, q. Wu, b. Luo, b. Zeng, m. Gabbouj, "noise-robust clustering description using local contrast patterns via global mea-sures", ieee signal process. Letters, vol. 21, no. 1, pp. 93-96, jan. 2014.
16. J. He, h. Ji, x. Yang, "rotation invariant clustering descriptor using local shearlet-based energy histograms", ieee signal process. Letters, vol. 20, no. 9, pp. 905-908, sep. 2013.
17. L. Zhang, z. Zhou, h. Li, "binary gabor pattern: an efficient and robust descriptor for clustering classification", pp. 81-84, sep. 2012.